Available online at www.sciencedirect.com
ScienceDirect
Applied Thermal Engineering 27 (2007) 848–861
Applied Thermal Engineering
www.elsevier.com/locate/apthermeng

# Modeling of internal combustion engine based cogeneration systems for residential applications

Hycienth I. Onovwiona [a], V. Ismet Ugursal [a,*], Alan S. Fung [b]

[a] Department of Mechanical Engineering, Dalhousie University, P.O. Box 1000 Halifax, NS, Canada B3J 2X4
[b] Department of Mechanical and Industrial Engineering, Ryerson University, Toronto, Ont., Canada M5B 2K3

Received 2 February 2006; accepted 15 September 2006
Available online 14 November 2006

**Abstract**

A parametric model that can be used in the design and techno-economic evaluation of internal combustion engine (ICE) based cogeneration systems for residential use is presented. The model, which is suitable to be incorporated into a building simulation program, includes sub-models for internal combustion engines and generators, electrical/thermal storage systems, and secondary system components (e.g. controllers), and is capable of simulating the performance of these systems in 15-min time steps. Water storage tanks for thermal storage and electrochemical (battery) systems for electrical storage are modeled. The parametric model provides users with useful information about the cogeneration system performance in response to a building's electrical and thermal demands. This paper presents the model, and the results of sensitivity analyses obtained using the model with a building simulation program. The results demonstrate the capabilities of the model and provide an insight into the energetic performance of ICE based cogeneration systems.
© 2006 Elsevier Ltd. All rights reserved.

*Keywords:* Residential cogeneration; Residential CHP; Micro-generation; Micro-cogeneration; Micro-CHP

## 1. Introduction

There is a growing potential for the use of cogeneration systems[1] in the residential sector because they have the ability to produce both useful thermal energy and electricity from a single source of fuel such as oil or natural gas, with the potential to reduce overall energy expenditure due to their higher energy conversion efficiency compared to that of conventional energy conversion systems. In cogeneration systems, the efficiency of energy conversion increases to over 80% (based on lower heating value, LHV[2]) as compared to an average of 30–35% for conventional fossil fuel fired electricity generation systems and up to 55% in combined cycle power plants, such as combined cycle gas turbine. This increase in energy efficiency can result in lower energy expenditures and reduction in greenhouse gas emissions when compared to the conventional methods of generating heat and electricity separately. The potential to reduce overall energy expenditures is especially critical for consumers considering the growing energy costs as prices for oil and natural gas continue to increase, at times in an unpredictable and/or volatile fashion.

Technologies suitable for residential cogeneration systems include reciprocating internal combustion engine (ICE), micro-turbine, fuel cell, and reciprocating external combustion Stirling engine based cogeneration systems. A comprehensive review and comparison of these systems is presented in Onovwiona and Ugursal [1] and Knight and Ugursal [2]. These reviews indicate that presently reciprocating internal combustion engines (ICE) are the prime mover of choice for residential cogeneration applications because of their well-proven technology, robust nature,

* Corresponding author. Tel.: +1 902 494 2246; fax: +1 902 423 6711.
*E-mail address:* Ismet.Ugursal@Dal.Ca (V. Ismet Ugursal).
[1] Also known as combined heat and power (CHP) systems.
[2] Many manufacturers Europe and Japan base engine power ratings in terms of the LHV of the fuel, in North America, the higher heating value (HHV) is usually used.

1359-4311/$ - see front matter © 2006 Elsevier Ltd. All rights reserved.
doi:10.1016/j.applthermaleng.2006.09.014

**Nomenclature**

| | | | |
|---|---|---|---|
| BSFC | brake specific fuel consumption | $P_{A,r}$ | adjusted rated power |
| $CF_a$ | correction factor for altitude and temperature | $P_r$ | rated power |
| $CF_t$ | correction factor for temperature | $P_e$ | electrical power output |
| DHW | domestic hot water | $Q_{th}$ | useful thermal output |
| EFFO | overall efficiency | SOC | state of charge |
| FU | useful thermal output | $t$ | time |
| HPR | heat to power ratio | $x$ | part load ratio |
| HHV | higher heating value | $\eta_o$ | overall efficiency |
| ICE | internal combustion engine | $\eta_Q$ | corrected thermal efficiency for cold start |
| LHV | lower heating value | $\eta_{Qmax}$ | thermal efficiency not affected by cold start |

reliability, and reasonable cost. However, they do need regular maintenance and servicing to ensure availability.[3] In addition to these advantages, the development of small household ICE cogenerators with low $CO_2$ and $NO_x$ emissions by several manufacturers have largely addressed emission concerns. For example Honda Motor Co.[4] has developed a 1 kW electrical and 3 kW thermal output cogeneration unit based on a natural gas fired internal combustion engine, specifically designed for single-family applications, and with a reported overall energy efficiency of 85% (based on LHV). Owing to the improvements in cogeneration technologies and potential for energy cost savings, the residential cogeneration market is beginning to develop in many parts of the world, including North America, Europe and Japan [1,2]. For example, in 2003, United States developed a micro-CHP roadmap, and is funding several micro-CHP programs, including those for the residential sector.[5]

The interaction between a building's electrical and thermal demands and a cogeneration unit represents a complex thermodynamic system because of factors such as the occupants' electrical and domestic hot water (DHW) usage patterns, the house's space heating demands, weather, the cogeneration plant performance characteristics and operational strategy, as well as the operation of other HVAC components. This complexity requires a building performance modeling and simulation tool that is capable of evaluating the thermal performance of the building and cogeneration plant as an integrated, dynamic system. Thus, this paper presents a comprehensive computer simulation model designed to be incorporated into a building energy simulation software, in this case the ESP-r [3], to be used in the design, techno-economic evaluation and optimization of ICE based cogeneration and associated thermal/electrical storage systems for residential use, as well as some illustrative results obtained using the model.[6] The model includes sub-models for ICE/generator unit, electrical (lead-acid battery) and thermal (hot water) storage systems, and secondary system components (e.g. controllers), and is capable of simulating the performance of these systems in a given time step. In this work, a time step of 15 min is used. Information regarding brake specific fuel consumption (BSFC), electrical efficiency, fuel flow rate and heating value, and engine exhaust temperatures of ICE based cogeneration units obtained from the literature, experimental and manufacturers' data was used to develop mathematical relationships that describe the effect of engine load on the engine electrical efficiency, thermal power, fuel consumption. and greenhouse gas emissions. Also, mathematical relations describing the cold start behavior of an engine and the effect of ambient temperature and altitude on engine performance were developed. A detailed presentation of the model and results demonstrating its capabilities are presented in Onovwiona [4].

## 2. ICE cogeneration system modeling

In this work, the ICE cogeneration system is assumed to address the space and domestic hot water heating and electrical loads of the residence; cooling loads are not considered. The conceptual design adopted for the residential ICE cogeneration system with electrical and thermal storage is presented in Fig. 1.

Two operating scenarios are assumed for the ICE cogeneration system. The *electrical priority controller* scenario involves operating the ICE to follow the electric demand of the building, while the *constant output controller* scenario involves operating the ICE at the minimum brake specific

[3] Reliability is determined by the amount of unscheduled outage as a result of equipment failure, while availability is the proportion of time the cogeneration plant is available for use when needed.

[4] http://world.honda.com/news/2001/p010830.html.

[5] Further information is available from the following websites:http://www.eere.energy.gov/de/pdfs/micro_chp_roadmap.pdf http://www.energetics.com/depeerreview05/agenda.html.

[6] ESP-r was selected due to its powerful energy flow modeling capabilities, as well as its capability to solve for the thermal and electrical flows and balances throughout an entire building. Its open source code allows for continual evolution and expansion of the original software kernel as developed and validated by the Energy Systems Research Unit at the University of Strathclyde [3]. ESP-r was selected by CANMET Energy Technology Centre (CETC) as the preferred simulation engine for future Canadian building simulation tools. Detailed information on ESP-r can be obtained from http://www.esru.strath.ac.uk/Programs/ESP-r.htm.

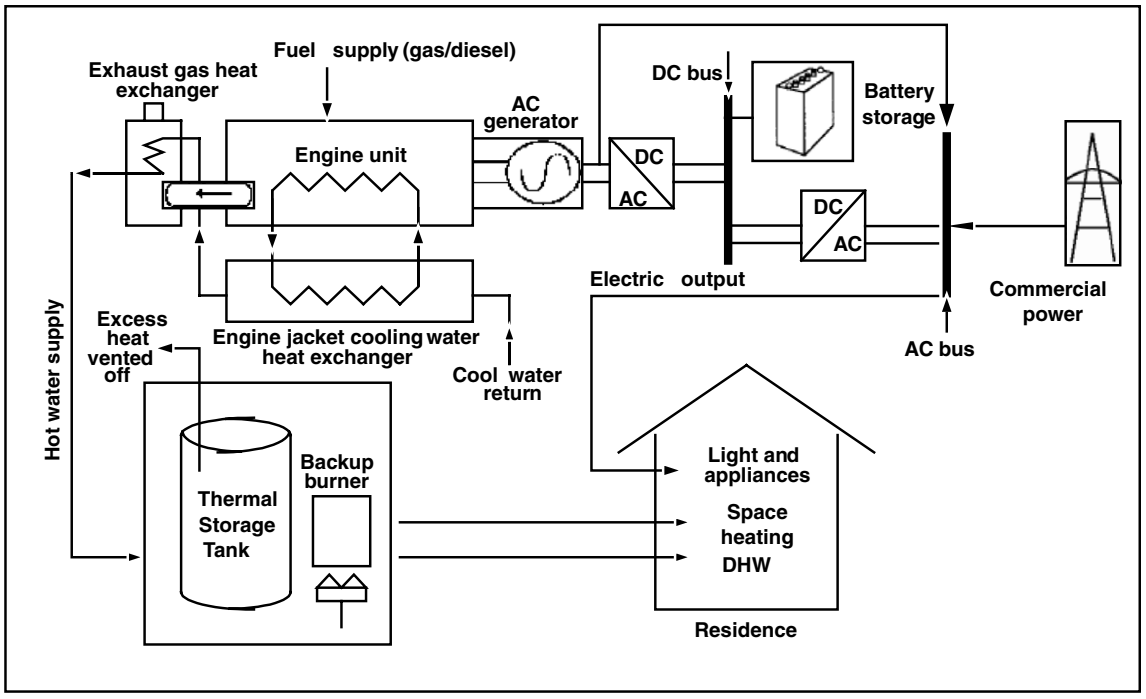


Fig. 1. A conceptual arrangement of residential ICE cogeneration system with thermal and electrical storage.

fuel consumption (BSFC) point, which coincides with operating the ICE at maximum electrical efficiency. With the *electrical priority controller*, the thermal energy derived from the ICE is used to meet the space and DHW heating energy demands, and any deficiency in meeting the electrical and thermal demands from the ICE is satisfied by the utility grid and a backup burner, respectively. The *constant output controller* involves the collaboration of the ICE and the battery block, where the surplus electricity from the ICE is stored in the battery block. It involves operating the ICE at maximum electrical efficiency, i.e. the ICE is started when the battery charge drops below a low-limit set point (25% is used here), and is operated at maximum efficiency (i.e. minimum BSFC point) until the battery charge reaches the high-limit set point, or until there is a deficit in the electrical network (i.e. the house's electrical load is higher than the electrical output from the ICE). At that instant, the ICE is switched off, and if the battery is able to satisfy the load, then it is used to supply the load. If the battery is unable to satisfy the electrical load, then the difference between the electrical load of the house and the battery contribution is purchased from the utility grid.

The thermal energy derived from the ICE is used to supply the building's heating loads. When the thermal output from the ICE is insufficient to meet the heating loads, the deficiency is satisfied by the backup burner. For both *electrical priority* and *constant output controller* scenarios, if excess heat is produced, the thermal storage is isolated from the system to avoid overcharging, and the excess heat is dumped into the environment.

The ICE cogeneration model consists of four sub-models. These are (1) an engine/generator unit model that predicts the electrical generation and heat production in response to changing building energy demands, taking into account the dynamic nature of both the electrical and thermal energy demands, and the operational characteristics and conditions of the ICE cogeneration system, (2) an electrical storage model that predicts the stored energy in the lead acid battery as a function of time, and the rate at which the battery is charged or discharged, (3) a thermal storage model that predicts the energy and mass flows in all other portions of the ICE cogeneration system including the performance of the auxiliary equipment such as the backup burner, and (4) power conditioning unit model that converts AC power to DC power, and DC power to AC power. Information from theoretical and experimental studies, and design, experimental and manufacturing data describing the characteristics of system components such as the ICE, controllers, battery and thermal storage devices are employed in model development. The space and domestic hot water heating, and electricity loads are predicted using the ESP-r building simulation program in time-step intervals based on the description of the building as well as the user defined domestic hot water and electricity load patterns and demands. The building thermal and electrical loads thus predicted (or actual load data from an existing building) are then employed in an annual simulation. The information flow structure of the model is shown in Fig. 2.

### 2.1. Internal combustion engine and generator model

There are two ways to model the behavior of an ICE. The explicit modeling approach involves modeling of the combustion process and thermodynamic cycle in detail

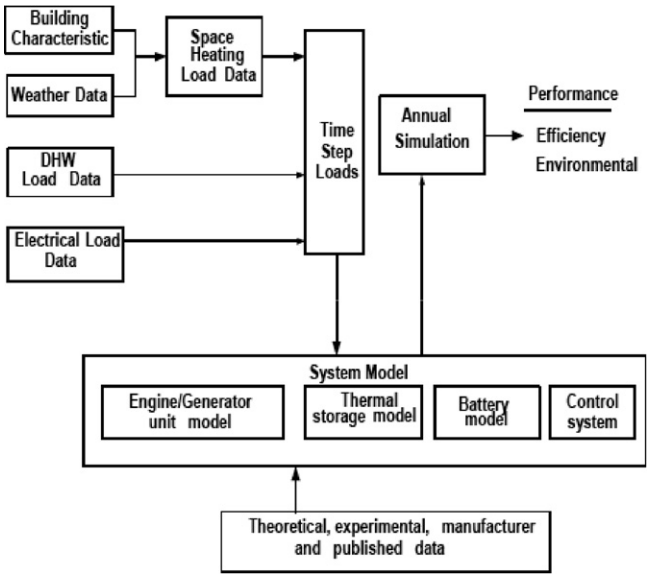


Fig. 2. Model information flow diagram.

(e.g. [5]). This approach requires in-depth expertise from its users, and a large volume of engine specific data that is difficult to obtain from manufacturers or by engine testing. Consequently, these models are not generic, and are difficult to use, making them unpractical for the purposes of this work. Therefore, a simplified parametric model based on performance data quoted by manufacturers is used here to predict the performance of an ICE with sufficient accuracy and precision. Performance characteristics of commercially available reciprocating ICEs with rated output in the 1–10 kW range suitable for residential application were collated and used in the development of the ICE model.

The engine and generator units of ICE based cogeneration systems are commonly manufactured as a single unit, and the performance information are often quoted for the overall unit (i.e. the performance of converting fuel to electricity). Therefore, to simplify the model, the ICE and the electrical generator are modeled as a single unit.

In cogeneration applications, the heat to power ratio (HPR) is obtained from

$$\mathrm{HPR} = Q_{\mathrm{th}}/P_{\mathrm{e}} \tag{1}$$

where $Q_{\mathrm{th}}$ is the useful thermal output and $P_{\mathrm{e}}$ is the electrical power output. The HPR must be determined, because heat and power are mutually exclusive and cannot be chosen independently. Therefore, the thermal power is mapped to the electric power output of the cogeneration system to determine the magnitude of the heat output that can be obtained for a given electric power output. The useful thermal power that can be utilized to satisfy a heating load can be determined from the fraction of useful thermal output (FU):

$$\mathrm{FU} = Q_{\mathrm{th}}/Q_{\mathrm{f}} \tag{2}$$

where $Q_{\mathrm{f}}$ is the primary fuel input. Thus, the overall efficiency ($\eta_{\mathrm{o}}$) of an ICE cogeneration system is

$$\eta_{\mathrm{o}} = (Q_{\mathrm{th}} + P_{\mathrm{e}})/Q_{\mathrm{f}} \tag{3}$$

In an ICE, if the percentage fuel energy input values for net work, exhaust and jacket water are summed at different percentage loadings, the overall percentage of fuel energy input which contributes to the net work, exhaust and jacket water outputs remains fairly constant. This implies that the overall efficiency (i.e. for electricity and heat) of an ICE cogeneration system remains fairly constant over the operating range of the engine. Thus, a constant value for the overall efficiency is assumed in this work. Based on this assumption, and the performance data from a 6 kW Cummins gas engine,[7] the variation of the specific fuel consumption, electrical efficiency and HPR are represented as a function of part load ratio

$$\mathrm{BSFC}\ (\mathrm{g/kW\,h}) = 966x^2 + 1767x + 1164 \tag{4}$$

$$\text{Electrical Eff.}\ (\%;\mathrm{HHV}) = -11.48x^2 + 29.11x + 2.58 \tag{5}$$

$$\mathrm{HPR} = -18.347x^3 + 45.76x^2 - 39.933x + 15.7 \tag{6}$$

where $x$ is the part load ratio, expressed as a decimal.

Due to the change in the density of air with altitude and temperature, the mass flow rate of air to an ICE changes with ambient temperature and site elevation. Correction factors derived from a one-dimensional steady compressible flow through an orifice [6] and manufacturer's data [7] are used here to adjust the rated power output for altitude and temperature changes from the standard ISO conditions of 25 °C and 1 bar pressure

$$P_{\mathrm{A,r}} = (P_{\mathrm{r}})(1 - \mathrm{CF_a} - \mathrm{CF_t}) \tag{7}$$

where $P_{\mathrm{A,r}}$ is the adjusted rated power, $P_{\mathrm{r}}$ is the rated power, and $\mathrm{CF_a}$ and $\mathrm{CF_t}$ are the correction factors for altitude and temperature, respectively, expressed as decimals. A derating of 3.5% per 300 m above 300 m above sea level is used as the correction factor for altitude, and 2% derating per 11°C above 25°C is used as the correction factor for temperature [8].

The transient behavior of an ICE during cold start operation has significant effect on the heat production, whereas for electricity generation, the transient behavior is negligible [9]. Therefore, the cold start behavior of an ICE, i.e. when the engine is started and stopped, and allowed to cool down before being started again, is modeled using equations developed by regression based on the experimental data published by Voorpools and D'haeseleer [9]. The equations are as follows:

Continuous operation:

$$\eta_{\mathrm{Q}}/\eta_{\mathrm{Qmax}} = 1 \tag{8}$$

Engine starts operation 1 h after shut-down:

$$\eta_{\mathrm{Q}}/\eta_{\mathrm{Qmax}} = -2 \times 10^{-8}t^2 + 0.0001t + 0.7824 \tag{9}$$

Engine starts operation 2 h after shut-down:

$$\eta_{\mathrm{Q}}/\eta_{\mathrm{Qmax}} = -5 \times 10^{-8}t^2 + 0.0003t + 0.5828 \tag{10}$$

[7] www.cumminspower.com.

Engine starts operation 4 h after shut-down:

$$\eta_Q/\eta_{Qmax} = -1 \times 10^{-7}t^2 + 0.0006t + 0.1692 \quad (11)$$

Cold start:

$$\eta_Q/\eta_{Qmax} = -8 \times 10^{-8}t^2 + 0.0005t + 0.0041 \quad (12)$$

where $\eta_Q$ is the corrected thermal efficiency for a particular engine load for cold start, $\eta_{Qmax}$ is the thermal efficiency corresponding to the same engine load when the engine is not affected by cold start, and $t$ is the operating time after cold start, expressed in seconds.

### 2.2. Electrical storage model

The charging, storing and discharging characteristics of lead acid batteries are used to develop the battery storage model. Lead acid batteries have the ability to accept, store and discharge electrical energy. The battery model is designed to calculate the stored energy in the lead acid battery as a function of time, and the rate at which the battery is charged or discharged. The model tracks the state of charge, SOC, (i.e. the instantaneous ratio of the actual amount of charge stored in the battery and the total charge capacity of the battery) according to the current drawn from or added to the battery. A charger controller is employed to regulate both the charging voltage and current to avoid damage from overcharging, and also to prevent over-discharging. The internal resistance of the battery is assumed to be the same during charging and discharging. The three stages involved in charging a lead acid battery, i.e. bulk charging at a constant current until voltage level rises to near 80–90% of full charge level; absorption charging where the battery voltage remains constant and the current is gradually reduced as the internal resistance increases; and float charging where the charging voltage is reduced to a lower level to prolong battery life by compensating for self-discharge, preventing a fully charged battery from overcharging, and reducing gassing [10] are addressed.

The model estimates the battery lifetime, self-discharge and temperature effects on battery performance, and utilizes data supplied by battery manufacturers, thus making the model accessible to a variety of users. It is assumed that many of the variables used in the battery model, including power output from the battery, is constant for each time step of the simulation. The state of charge (SOC) is calculated as a function of both the rate of current in or out, and the previous time step SOC, which in turn is used to determine the open circuit voltage of the battery (i.e. when the battery current is zero). Further details of the electrical storage models are presented in Onovwiona [4].

### 2.3. Thermal storage model

While sensible and/or latent heat storage can be used, only sensible heat storage is considered in this work. The quantity of energy stored by a sensible heat storage device depends on the mass and the specific heat of the storage medium (i.e. the heat capacity of the storage medium), and the temperature difference between the initial and final temperatures in a given time step. Water is the most widely used material for sensible-heat storage since it is relatively easy and inexpensive to store water at temperatures up to 150–200 °C if pressurized tanks are used. In this study, it is assumed water is stored at a temperature between 50 °C and 75 °C. The fully-mixed thermal storage tank model developed by Beausoleil-Morrison [11] for the ESP-r platform is used to model the thermal storage tank.

## 3. Model application and results

The ICE cogeneration model was implemented within the ESP-r building simulation program using FORTRAN 77 programming language, and was used to simulate the performance of an ICE cogeneration system in an R-2000 house.[8] The integrated building energy simulation used to demonstrate the application of the ICE cogeneration system model consists of

- a building model representing the physical structure of the building,
- an HVAC plant network model that produces and distributes the heat required by the building,
- ICE and battery models that produce, distribute and store the electrical energy required by the building,
- models representing control systems that activate the HVAC plant network and battery block in response to building loads.

The HVAC plant was connected to an existing building model meeting the R-2000 standard. The building model used for this work is based on the previous work of Purdy and Beausoleil-Morrison [12], which examined a modern, energy efficient house constructed at the Canadian Centre for Housing Technology (CCHT) in Ottawa, Canada. The wood-frame construction house built upon a concrete foundation comprises two above-grade storeys and a conditioned basement. Its size is typical of a modern Canadian suburban construction, with 240 $m^2$ conditioned floor area (excluding basement area) and well insulated. The house is divided into four zones, and was simulated using the weather file for Montreal. Control schemes were devised to operate the HVAC plant network and battery block, and models representing these control schemes were developed. The total building thermal load, including space and DHW heating was found to be 71.3 GJ/year.

[8] R-2000 is Canadian home building technology with a worldwide reputation for energy efficiency and environmental responsibility. The R-2000 Standard is a series of technical requirements for new home performance. Every R-2000 home is built and certified to this standard. See http://r2000.chba.ca/ for details.

ESP-r's building thermal domain determines the thermal demands placed upon the ICE cogeneration system on a time-step basis while the electrical demands placed upon the ICE are user specified. The DHW draw schedule and dwelling's non-HVAC electrical loads are representative of a family of four. At each time-step of the simulation, the non-HVAC electrical load is read from the data input file and the ICE is controlled to respond to this demand. The non-HVAC electrical load includes the total load generated by lighting, appliances, home entertainment, and other equipment. A subroutine in *ESP-r* calculates the demand imposed by the HVAC equipment (pumps, fans, compressors), and this forms part of the total electrical load.

An HVAC plant network was formed by combining the ICE model with the existing *ESP-r* component models for the gas-fired water storage tank, pumps, pipes, and fans as illustrated in Fig. 3. Water is extracted from the gas fired hot water tank by a pump attached to the storage tank and passed through the heat exchanger circuit (i.e. combined unit of engine jacket and exhaust heat exchangers) of the ICE cogeneration system where the thermal output of the ICE is transferred to the water before being fed back to the water storage tank. The water storage tank is directly used to supply the dwelling's DHW needs while the fan coil attached to the storage tank is used to supply the space heating requirements. A second pump circulates hot water from the storage tank to the fan coil.

The backup burner is activated when the tank temperature drops below 50 °C and it is turned off at 60 °C. Thus, the burner cycles on when the ICEs thermal output is insufficient to meet the space heating and DHW requirements. A safety device regulates the temperature in the storage tank by extracting heat from the tank and discharging it to the environment when the ICEs thermal output exceeds the dwelling's space heating and DHW requirements, as well as the tank's ability to store this energy. Heat rejection starts when tank temperature rises above 75 °C, and stops when the temperature drops to 70 °C.

### 3.1. Results – electricity priority controller

With this control mode, the ICE is operated to match the electrical demand from the building, i.e. the ICEs electrical output is varied throughout the simulation period to follow the electrical load, and the thermal output is stored in the water storage tank if it has thermal capacity. The key aspects of the ICEs performance for the annual simulation are illustrated in Figs. 4 and 5. Fig. 4 compares the inlet and outlet exhaust gas temperatures of the exhaust heat exchanger over the full simulation period and shows the temperature range for the final hot water temperature leaving the exhaust heat exchanger. As can be seen, the temperature of the inlet exhaust gases entering the heat exchanger is between 330 °C and 585 °C over the ICEs operating range while the temperature of the exhaust gases exiting the heat exchanger range from 125 °C to 190 °C. The average temperature drop of the gases through the heat exchanger is 315 °C. These temperatures conform to the exhaust gas temperature range derived from Cummins data and literature [13].

Fig. 5 compares the ICEs thermal and electrical output, and shows the useful thermal output extracted from the ICE. This figure illustrates that the heat to power (HPR) ratio is 8.6 at the lower end and 2.8 at the upper end of the ICEs operating range. The average HPR ratio over the annual simulation period is 5.0. In addition, the heat to fuel ratio at the lower end is 0.61, and 0.56 at the upper end. These results show that more fuel is required per kW h of electricity at the lower end (i.e. lower engine efficiency) and the amount of heat generated from the engine jacket cooling water and exhaust gases increases as the engine load drops. These results are as expected.

The thermal state of the water tank (i.e. 300 kg capacity including tank casing) and the state of the hot water leaving the ICE are illustrated in Fig. 6 for the period commencing at midnight on January 1st and ending at midnight on January 3rd. Fig. 6 plots the tank temperature

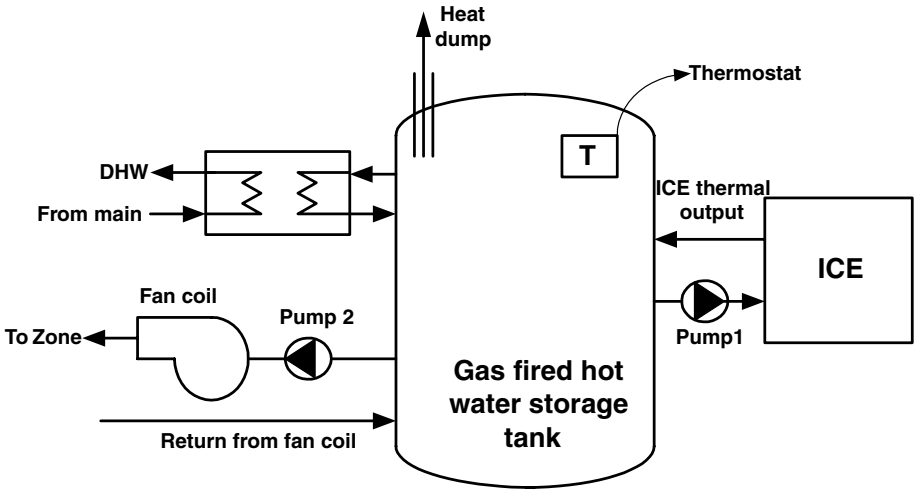


Fig. 3. HVAC plant network.

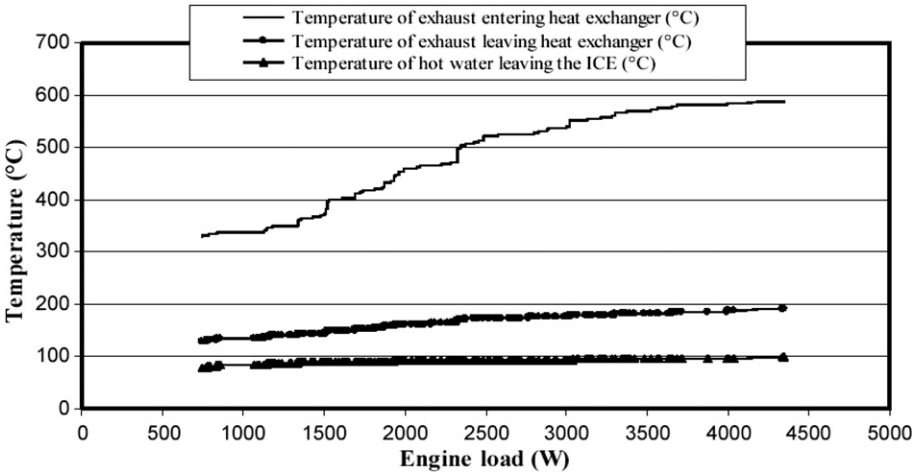


Fig. 4. ICE cogeneration control volume temperatures.

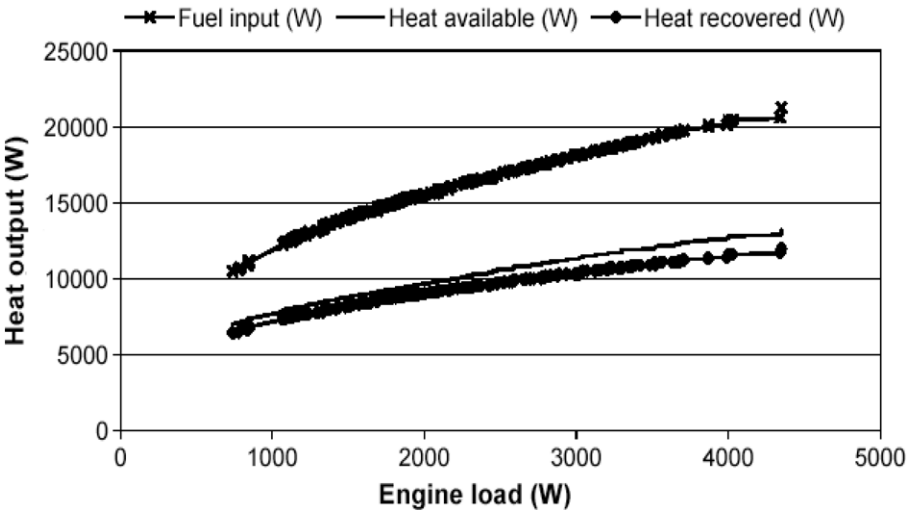


Fig. 5. Heat balance of the ICE cogeneration system.

and hot water temperature leaving the ICE. During this period, the tank water temperature is above the lower limit of the burner's set point (50 °C in this case), resulting in the burner to be inactive. The variations seen in the tank temperature and the temperature of the hot water leaving the ICE is due to DHW and space heating draws. Fig. 6 also shows how the safety device is activated frequently (i.e. when the tank temperature rises above the safety limit of 75 °C).

The overall energy balance of the ICE cogeneration unit is shown in Fig. 7 where the monthly thermal and electrical output of the ICE as well as the thermal output of the backup burner are plotted. Owing to the control scheme employed for this simulation, the ICEs thermal and electrical outputs are nearly constant over the year. The burner contribution during the heating season is small, and the burner is completely inactive from May through September (i.e. during the summer months) when the heating system is shut off.

The overall thermal energy balance of the 300 kg capacity thermal storage tank is illustrated in Fig. 8 where the monthly energy inputs to the water tank and the energy dumped through the storage tank's safety device are plotted. The burner contribution during the heating season is minimal, and the burner is completely inactive from May through September. The only draws on the tank during this period are for DHW. Thus, during the summer months, the ICEs thermal output is sufficient to meet all DHW requirements. Fig. 8 also shows the overall magnitude of the heat dumped throughout the year. This is because the ICEs thermal output substantially exceeds the house's space heating and DHW requirements, and the water storage tank is unable to store all of the excess thermal output of the ICE. A smaller capacity engine would result in a reduced heat dump.

Overall simulation results for a 6 kW capacity engine operated under the *electrical priority controller* scenario are summarized in Table 1. These results indicate that the

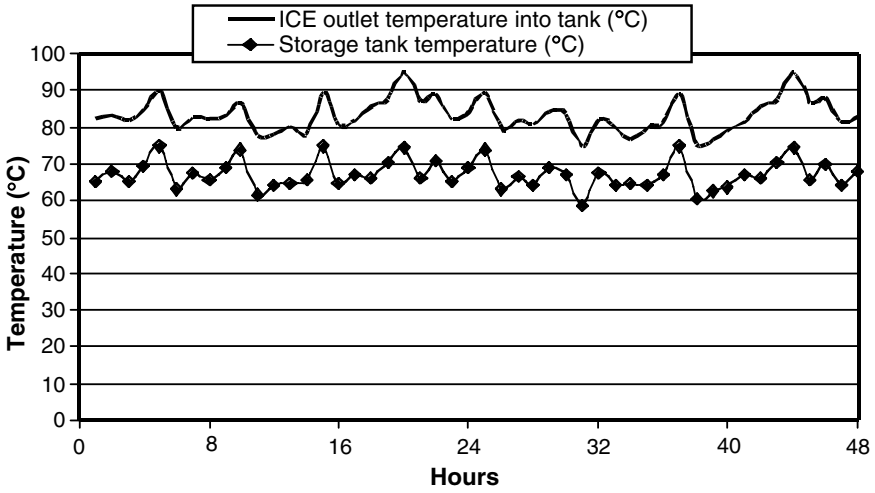


Fig. 6. Temperature of the water in the storage tank and the temperature of the hot water leaving the ICE in January, electrical priority controller configuration.

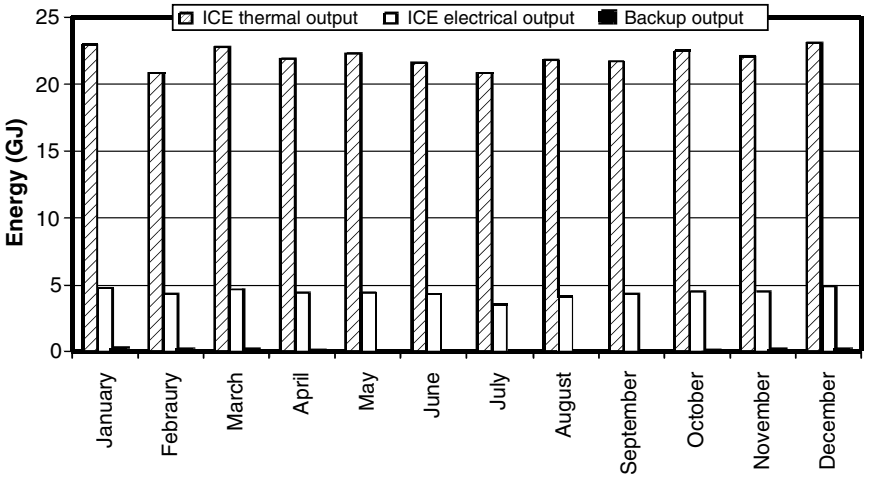


Fig. 7. Monthly energy balance of the ICE cogeneration unit, electrical priority controller configuration.

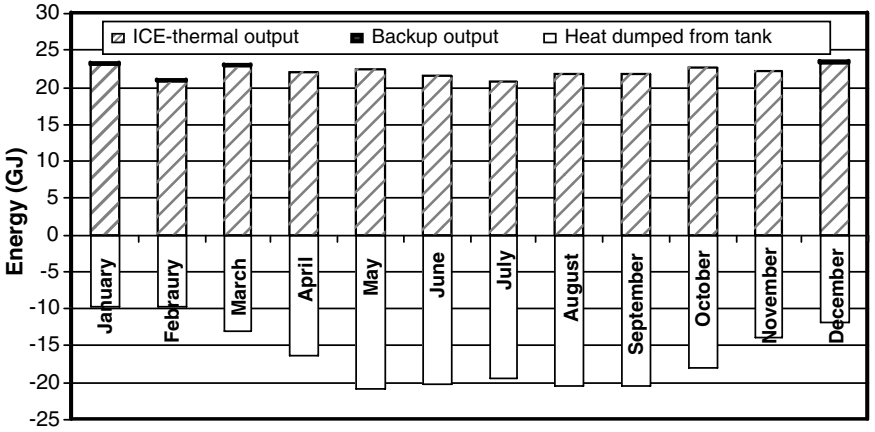


Fig. 8. Monthly energy balance on water storage tank, electrical priority controller configuration.

ICE responds to 98% of the house's total thermal and 100% of the house's electrical demand. Due to the size of the engine used (6 kW), and the inability of the tank to accommodate most of the thermal energy produced by the ICE, significant amount of thermal energy is dumped from the storage tank. The overall efficiency of the ICE

Table 1
Annual simulation results with 2 kW, 3.5 kW and 6 kW capacity ICE cogeneration systems with electrical priority controller (efficiencies based on HHV)

| | | | |
|---|---|---|---|
| ICE capacity (kW) | 6 | 3.5 | 2 |
| ICE thermal output to tank (GJ) | 264 | 187 | 131 |
| Energy rejected from tank[a] (GJ) | 194 | 121 | 78.7 |
| ICE net thermal contribution (GJ) | 70 | 66 | 52.3 |
| Backup burner output[b] (GJ) | 0.03 | 4 | 17.8 |
| Back-up burner seasonal efficiency (%) | 85 | 85 | 85 |
| Back-up burner fuel requirement, HHV (GJ) | 0.035 | 4.7 | 21 |
| Fan coil internal heat generation (GJ) | 1.16 | 1.3 | 1.3 |
| Backup contribution (burner + fan coil) (GJ) | 1.18 | 5.3 | 19 |
| ICE electrical contribution (kW h) | 14,639 | 14,556 | 13,083 |
| ICE fuel requirement (GJ) | 452 | 324 | 228 |
| House thermal energy requirement (GJ) | 71.3 | 71.3 | 71.3 |
| House electrical energy requirement (kW h) | 14,639 | 14,639 | 14,639 |
| Purchased electricity (kW h) | 0 | 146 | 1610 |
| Overall efficiency of ICE system assuming dumped heat is used for a useful purpose[c] (%) | 70 | 74 | 78 |
| Overall efficiency of ICE system assuming dumped heat not used for a useful purpose (%) | 27 | 37 | 43 |
| Average ICE electrical efficiency (%) | 11.2 | 15.5 | 20.3 |
| Electrical efficiency at full capacity (%) | 23.3 | 23.3 | 23.3 |

[a] Heat rejected = ICE thermal out + backup contribution (burner + fan coil) − building's thermal load.
[b] The parasitic loss from the storage tank was accounted for in the simulation.
[c] The overall efficiency is the sum of the ICE thermal output and the ICE electrical output divided by the fuel input.

system assuming the dumped heat can be used for a useful purpose agrees with the overall efficiency range obtained for ICE cogeneration systems. The average ICE electrical efficiency indicates that the ICE was operated mostly at part load during the simulation period resulting in more fuel being consumed per kW h of electricity.

### 3.2. Results – constant output controller

In this scenario, the ICE control loop is configured to maintain the ICE system's electrical production at a constant 6 kW output. This scheme involves the collaboration of the ICE and the battery block, where the surplus electricity from the ICE is stored in the battery block.

Fig. 9 shows the hourly backup burner thermal contribution to the storage tank when the ICE is inactive, and the hourly ICEs thermal contribution when the ICE is active. During the period when the ICE is active, the thermal output from the ICE is sufficient to meet the building's thermal loads, requiring no backup heat. The tank temperature and the temperature of the hot water leaving the ICE are plotted in Fig. 10 for the period commencing at midnight on January 1st and ending at midnight on January 3rd. During the period when the ICE is inactive, the burner is used to supply the house's heating requirements. When ICE is off, the tank's burner cycles on whenever the water temperature drops below 50 °C and stays on until the upper limit of the burner's set point of 60 °C is achieved. The tank cools down when the burner is not operational due to DHW and space heating draws.

Fig. 10 also shows how the safety device is activated frequently as the tank temperature rises above the safety limit of 75 °C when the ICE is operating. This is because the ICEs thermal output exceeds the house's space heating and DHW requirements, and the inability of the storage water tank to store the excess thermal output of the ICE. As seen in Fig. 10, the ICE outlet temperature follows the water storage tank temperature when the ICE is inactive. This is because the ICE and water storage tank are part of the HVAC network and the water still flows through the ICE even though the ICE is not operating.

The hourly ICE thermal output and backup thermal output compared to the hourly space heating and DHW requirements of the house are illustrated in Fig. 11 where the hourly heat recovered from the ICE, the thermal output of the backup heater, as well as the house's space heating and DHW requirements for the period commencing at midnight on January 1st and ending at midnight on January 2nd are plotted. It is seen that when the ICE is operating, its thermal output exceeds the house's space heating and DHW requirements, and the burner is inactive during

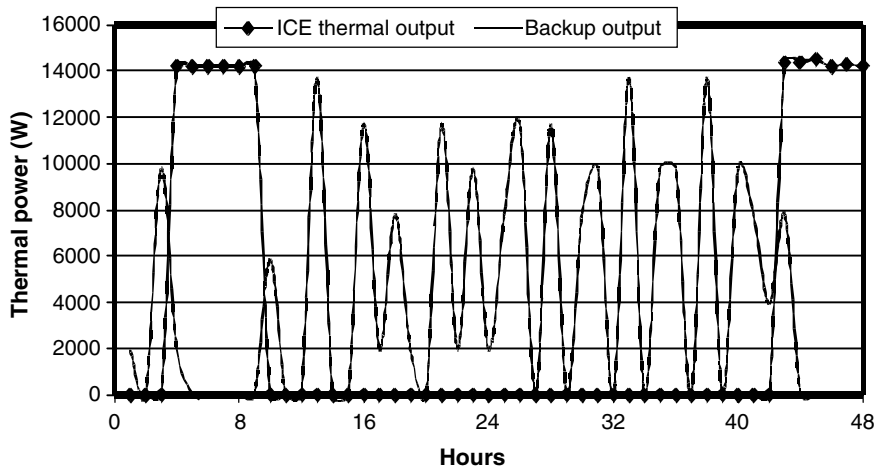


Fig. 9. ICE and backup thermal contributions (zero thermal output indicates that the ICE is not operational), constant output controller configuration.

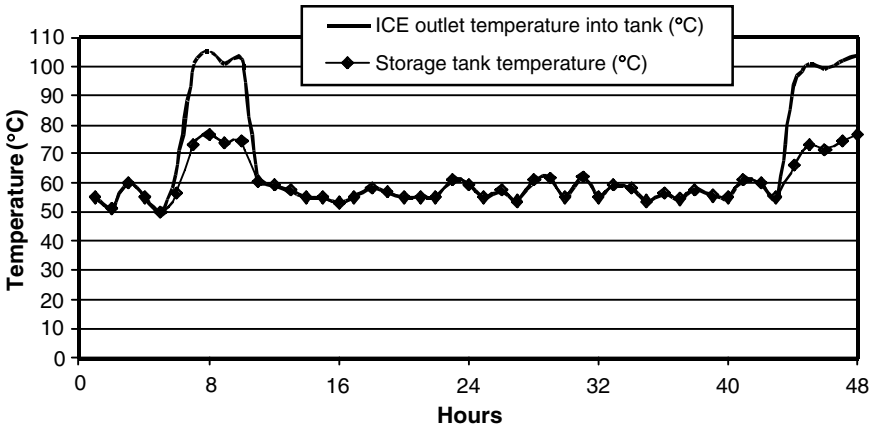


Fig. 10. Temperatures of water in storage tank and hot water leaving the ICE in January, constant output controller configuration.

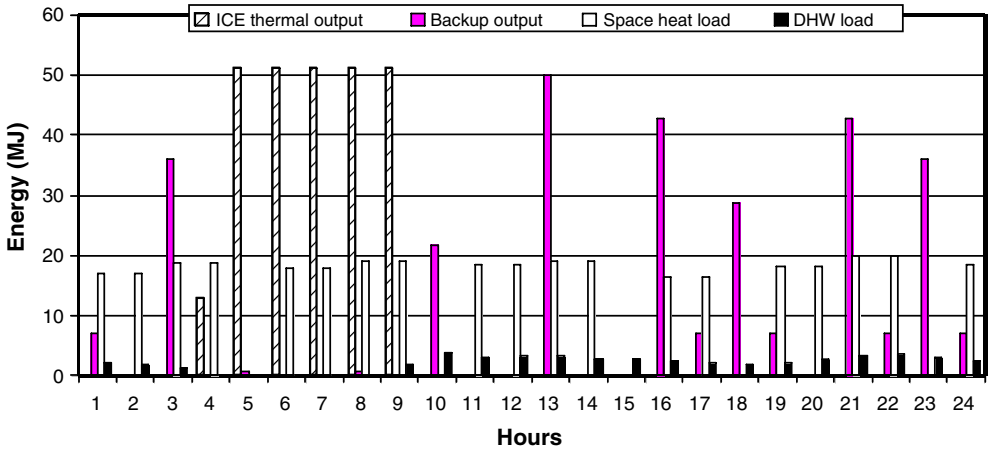


Fig. 11. Hourly heat flux, constant output controller configuration.

this period. The only heat generated by the backup during this period is the internal heat generated by the fan coil. On the other hand, when the ICE is off, the burner together with the fan coil supply the house's space heat and DHW requirements.

The ICEs hourly electrical output, the power flow supplied to the battery, and the battery output supplied to the electrical load compared to the hourly electrical load requirement of the house are illustrated in Fig. 12 for the period commencing at midnight on January 1st and ending

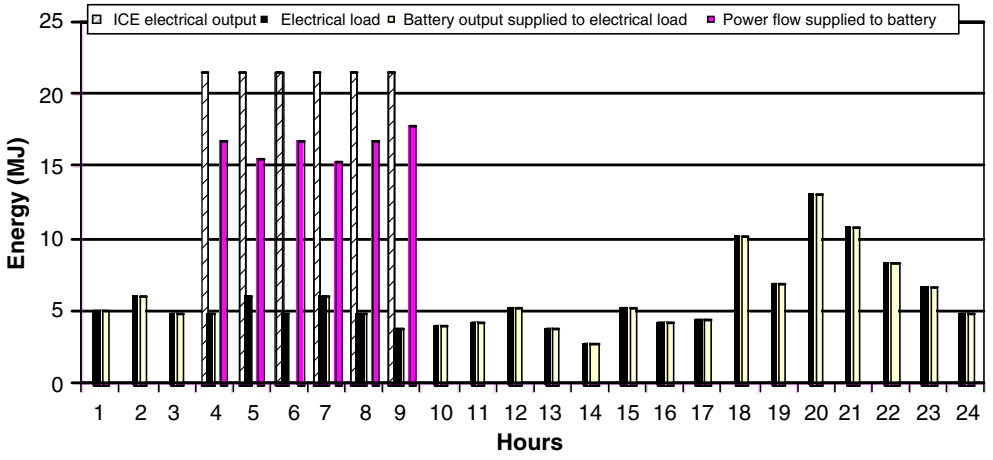


Fig. 12. Hourly electrical output, constant output controller configuration.

at midnight on January 2nd. No electricity needs to be purchased because the battery block was sized to cover one-day period of the building's electrical demand. As can be seen, when the ICE is operating, it is used to meet the house's electrical load and charge the battery at the same time. On the other hand, when the ICE is switched off, the battery supplies the house's electrical load.

Fig. 13 shows the overall energy balance of the ICE cogeneration unit for the constant output controller where the monthly thermal and electrical outputs of the ICE, the battery output supplied to the electrical load, and the backup thermal output are plotted. As can be seen, the ICEs thermal output and electrical output as well as the battery output supplied to the electrical load are nearly constant over the year. This is consistent with the on/off control scheme employed. The heat produced from the backup burner is minimal during the summer months when compared to the ICEs thermal output and the backup heat produced during the winter months. This is because there is no space-heating requirement during this period and this heat is used only for DHW.

The overall thermal energy balance of the thermal storage tank using the constant output controller is illustrated in Fig. 14 where the monthly energy inputs to the water storage tank as well as the energy dumped through the storage tank's safety device are plotted. The backup heater provides a significant amount of energy during the heating season, while during the summer months, this contribution is minimal when compared to the ICEs thermal output. This is attributed to the ICE meeting 90% of the DHW load during the summer months when there is no space heating load.

Simulation results for a 6 kW capacity engine operated under the constant output controller scenario summarized in Table 2 indicate that the ICE responds to 61% of the house's total thermal requirements and 100% of the house's electrical demand while the backup burner responds to 39% of the house's total thermal requirements. Forty nine

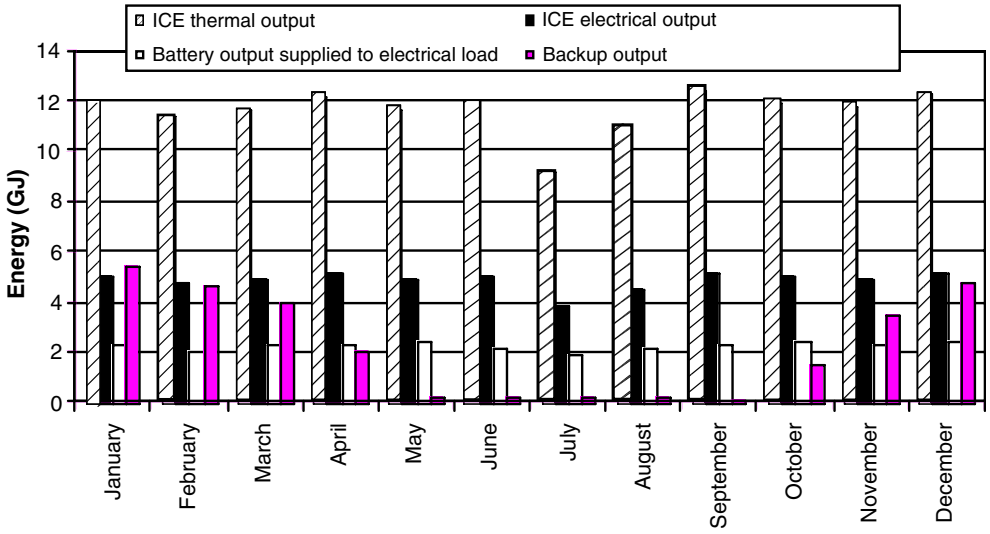


Fig. 13. Monthly energy balance of the ICE cogeneration unit, constant output controller configuration.

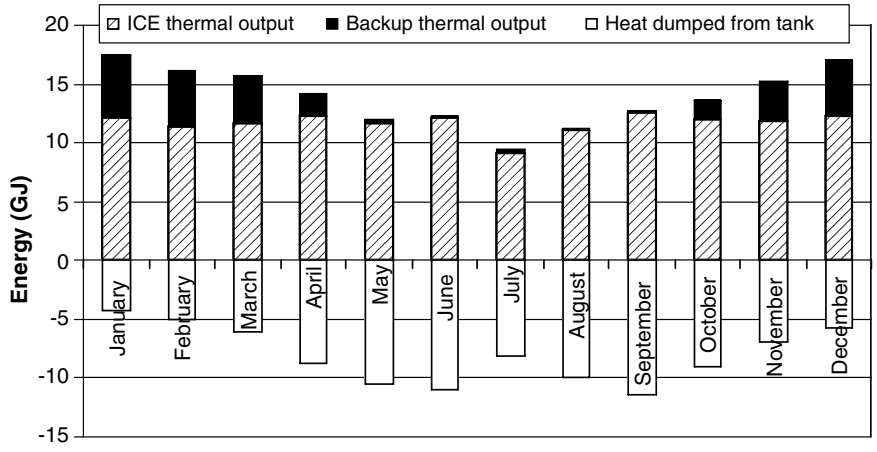


Fig. 14. Monthly energy balance on water storage tank, constant output controller.

Table 2
Annual simulation results with 2 kW, 3.5 kW and 6 kW capacity systems with constant output controller (Efficiencies based on HHV)

| | | | |
|---|---|---|---|
| ICE capacity (kW) | 6 | 3.5 | 2 |
| ICE thermal output to tank (GJ) | 140 | 139 | 136 |
| Energy rejected from tank[a] (GJ) | 96.3 | 94.3 | 87.5 |
| ICE net thermal contribution (GJ) | 43.7 | 44.6 | 48.4 |
| Backup burner output[b] (GJ) | 26.4 | 25.5 | 21.7 |
| Back-up burner seasonal efficiency (%) | 85 | 85 | 85 |
| Back-up burner fuel requirement (GJ) | 31 | 30 | 25.5 |
| Fan coil internal heat generation (GJ) | 1.19 | 1.21 | 1.24 |
| Backup contribution (burner + fan coil) (GJ) | 27.6 | 26.7 | 22.9 |
| Gross electrical output (kW h) | 16,222 | 16,128 | 15,578 |
| ICE electrical contribution (kW h) | 7167 | 7972 | 10,444 |
| ICE fuel requirement (GJ) | 249 | 247 | 239 |
| Battery bank contribution (kW h) | 7556 | 6750 | 3984 |
| House thermal energy requirement (GJ) | 71.3 | 71.3 | 71.3 |
| PCU loss (kW h) | 1500 | 1406 | 1150 |
| House electrical energy requirement (kW h) | 14,722 | 14,722 | 14,722 |
| Overall efficiency of ICE system assuming dumped heat is used for a useful purpose[c] (%) | 79.6 | 80 | 80.5 |
| Overall efficiency of ICE system assuming dumped heat not used for a useful purpose (%) | 41 | 42 | 44 |

[a] Heat rejected = ICE thermal out + backup contribution (burner + fan coil) − building's thermal load.
[b] The parasitic loss from the storage tank was accounted for in the simulation.
[c] The overall efficiency is the sum of the ICE thermal output and the ICE electrical output divided by the fuel input.

percent of the total electrical requirement (25.8 GJ) is supplied directly by the 6 kW ICE, whereas 51% (27.2 GJ) is supplied indirectly through the battery storage. Heat dumps from the storage tank only occur during cooling season (i.e. summer months). The overall efficiency of ICE system assuming the dumped heat can be used for a useful purpose agrees with the overall efficiency range obtained for ICE cogeneration systems. The annual fuel consumption is significantly reduced when the ICE is used together with the battery storage. With the *constant output controller* there is a fuel saving of 45% compared to the *electrical priority controller*.

### 3.3. Results – sensitivity analysis

To quantify the response of the ICE based cogeneration system to variations in the size of key system components, ICE and thermal storage sizes were varied, and the behavior of the model predictions were observed. Sensitivity analyses were carried out for both control scenarios (i.e. *electrical priority* and *constant electrical output controllers*).

#### 3.3.1. Electrical priority controller

The results of the analysis for varying ICE size with the electrical priority controller are given in Table 1. As can be seen from Table 1, the 6 kW capacity ICE system responds to 98% of the house's total thermal requirements and 100% of the house's electrical demand while the 3.5 kW ICE system responds to 93% of the house's total thermal requirements and 99% of the house's electrical demand. The 2 kW capacity ICE responds to 73% of the house's total thermal requirements and 89% of the house's electrical demand. 1% and 11% of the house's total electrical requirements were purchased from the grid using the 3.5 kW and 2 kW ICE systems, respectively.

The results in Table 1 indicate that the 6 kW capacity ICE cogeneration system is not utilized to its full potential in the house used in the simulations, resulting in poor annual efficiencies, both electrical, and combined electrical and thermal. Due to the large size of the 6 kW system for the house, and the inability of the tank to accommodate most of the thermal energy produced by the ICE, a significant amount of thermal energy has to be rejected from the storage tank compared to the other two ICE systems with 2 kW and 3.5 kW capacities. With the 2 kW capacity ICE, most of the heat rejection from the tank occurs during the summer months, and the overall heat rejection is significantly lower compared to the 3.5 kW and 6 kW capacity ICE systems.

The overall efficiency values obtained for the three ICE systems assuming the dumped heat can be used for a useful purpose agrees with the overall efficiency range reported for ICE cogeneration systems. The average ICE electrical efficiency for the 2 kW capacity ICE system indicates that the ICE was operated closer to the minimum specific fuel consumption point compared to the 6 kW and 3 kW capacity systems, resulting in lower fuel consumption. Therefore, the 2 kW capacity ICE system is more efficient for this application compared to the 3.5 kW and 6 kW capacity systems. This is reflected in the savings in total fuel consumption (i.e. savings in the total ICE and backup burner fuel consumption) obtained with the 2 kW system. The 2 kW system produces fuel savings in the order of 24% and 45% compared to the 3.5 kW and 6 kW systems, respectively, indicating the importance of proper selection of system capacity for a given application.

#### 3.3.2. Constant electrical output controller

The results of the analysis for varying ICE size with the constant output controller are given in Table 2. As can be seen from this table, the 6 kW ICE system responds to 61% of the house's total thermal requirements and 100% of the house's electrical demand, while the backup burner responds to 39% of the house's total thermal requirements. Forty eight percent of the total electrical requirement is supplied directly by the 6 kW ICE, whereas 52% is supplied indirectly through the battery storage. The 3.5 kW ICE responds to 63% of the house's total thermal requirements while the backup burner responds to 37% of the house's total thermal requirements. 54.4% of the total electrical requirement is supplied directly by the 3.5 kW ICE whereas 45.6% is supplied indirectly through the battery storage. Similarly, the 2 kW ICE responds to 68% of the house's total thermal requirements while the backup burner responds to 32%. Seventy one percent of the total electrical

requirement is supplied directly by the 2 kW ICE whereas 27% is supplied indirectly through the battery storage. Two percent of the house's total electrical requirement is purchased from the grid using the 2 kW ICE. The results in Table 2 indicate that significant amounts of thermal energy are rejected to the environment with all three ICE systems. The 6 kW ICE system rejects more heat to the environment than the other two systems, while the 2 kW system rejects the least. With a larger thermal storage, it would be possible to store more of the heat.

The overall efficiency values obtained for the three ICE systems assuming the dumped heat can be used for a useful purpose agrees with the overall efficiency range reported for ICE cogeneration systems. The average ICE electrical efficiency for the 2 kW capacity ICE system indicates that the ICE was operated closer to the minimum specific fuel consumption point compared to the 6 kW and 3.5 kW capacity systems, resulting in lower fuel consumption. Therefore, the 2 kW capacity ICE system is more efficient for this application. This is reflected in the savings in total fuel consumption (i.e. savings in the total ICE and backup burner fuel consumption) obtained with the 2 kW system. The 2 kW system produces fuel savings in the order of 4.6% and 5.7% compared to the 3.5 kW and 6 kW systems, respectively, indicating the importance of proper selection of system capacity for a given application.

The results of the simulations conducted with the two control strategies, i.e. the *constant output controller* and the *electrical priority controller* indicate that there are large differences in the performance of the ICE cogeneration systems due to the control scheme employed. As shown in Tables 1 and 2, with the 6 kW capacity ICE system, the annual fuel consumption with the *constant output controller* was significantly reduced, resulting in 45% fuel savings, compared to using the *electrical priority controller*. Although more fuel was consumed by the backup burner in generating heat, especially during the period when the ICE is inactive, operating the ICE cogeneration system under the *constant output controller* is more efficient compared to operating it under the *electrical priority controller*. With the 3.5 kW system, the savings were less, but still substantial (i.e.16%). However, with the 2 kW capacity, the *electrical priority controller* is more efficient compared to operating it under the *constant output controller*, resulting in 6% fuel saving.

Part of the reason for the reduced energy consumption is due to the reduced amount of heat rejected to the environment. For example, as seen in Tables 1 and 2, with the 6 kW capacity system, the amount of heat rejected with the *constant output controller* is 96.3 GJ, whereas with the *electrical priority controller*, this amount is 194 GJ. The amount of heat rejected with the 6 kW system corresponds to 31% of the thermal energy produced by the ICE operated under the *constant output controller* compared to 73% for the *electrical priority controller*.

These results indicate that to determine the preferable operation mode, an analysis needs to be conducted. Additionally, the assumptions regarding the PCU performance can have a significant impact on the results.

## 4. Conclusion

In this work, a model was developed within the ESP-r building simulation program for ICE based residential cogeneration systems with thermal and electrical storage. Two operating scenarios for the control of the thermal and electrical storage and the ICE are included in the model. The model is useful for conducting technical and economic evaluation of ICE based cogeneration systems, and as a research and development tool for assessing and optimizing system design variables. Sample results obtained using the model were presented to illustrate the operation and flexibility of the model. The results indicate the importance of the proper selection of the size of the ICE, the capacity of thermal and electrical storage systems and the operation scenario on the energetic performance of the entire system in a given application.

## Acknowledgements

The authors gratefully acknowledge the financial support provided by the Building Simulation University Research Network, Natural Resources Canada, and Natural Sciences and Engineering Research Council Canada. The authors are also grateful for the contributions of the researchers and the Head (Dr. I. Beausoleil-Morrison) of the Building Simulation Research Group at CANMET Energy Technology Centre, Natural Resources Canada, as well as the valuable comments of an anonymous reviewer.

## References

[1] H.I. Onovwiona, V.I. Ugursal, Residential cogeneration systems: review of the current technology, Renewable and Sustainable Energy Reviews 10 (5) (2005) 389–431.
[2] I. Knight, V.I. Ugursal, Residential cogeneration systems: a review of the current technologies, A Report of Annex 42 of the International Energy Agency, Energy Conservation in Buildings and Community Systems Programme, April 2005.
[3] ESRU, The ESP-r system for building energy simulations: user guide version 9 series, ESRU Manual U00/1, University of Strathclyde, Glasgow UK, 2000.
[4] H.I. Onovwiona, Modeling of reciprocating internal combustion engine based cogeneration system for residential applications, MASc Thesis, Dalhousie University, Halifax, 2005.
[5] N.J. Kelly, Towards a design environment for building integrated energy systems: the integration of electrical power flow modeling with building simulation, PhD thesis, Department of Mechanical Engineering ESRU, University of Strathclyde, Glasgow, 1998.
[6] J.B. Heywood, Internal Combustion Engine Fundamentals, McGraw-Hill, New York, 1988.
[7] Cummins Power Generation. Spark-Ignited Generator Set, Model GNAA 60 Hz. http://www.cumminspower.com/Commercial1/Spark-Ignited/S-1179.pdf, 2004 (accessed 13.10.04).
[8] Energy Nexus Group, Technology characterization: Reciprocating engines Environmental protection agency, Washington, DC, 2002.

[9] K.R. Voorpools, W.D. D'haeseleer, The evaluation of small scale cogeneration for residential heating, Int. J. Energy Res. 26 (2002) 1175–1190.
[10] Buchmann, Isidor. Batteries in a portable world. http://www.buchmann.ca, 2001 (accessed 13.10.04).
[11] I. Beausoleil-Morrison, Design of storage tank component models for FCT project, NRCan CETC Report, 2001.
[12] J. Purdy, I. Beausoleil-Morrison, The significant factors in modeling residential buildings, in: Proc. 7th Int. IBPSA Conf. on Building Simulation, 13–15 August 2001, Rio de Janeiro.
[13] ASHRAE. HVAC systems and equipment, SI Edition, American Society of Heating, refrigerating and Air-Conditioning Engineers Inc, Atlanta USA, 1996.